An Advanced Simulation Model for Brushless DC Motor Drives

B. K. Lee
Member, IEEE

M. Ehsani
Fellow, IEEE

Texas A&M University
Dept. of Electrical Engineering
College Station, TX 77843-3128, U.S.A

Abstract- **A dynamic simulation model for the brushless dc (BLDC) motor drives using Matlab is presented. In this model, an entire BLDC motor drive, including power conversion unit, BLDC motor, and speed/torque control system, is investigated. Especially, the PWM inverter is modeled using switching function concept, so that the detailed voltage and current waveforms, such as line-to-line voltages, inverter input current, ac line current, and switch/diode currents, can be obtained and average/rms ratings of the components can be easily calculated. Also, the proposed model is made into modular blocks and it can be easily extended to other ac motor applications with a little modification. The detailed modeling method is explained and its actual implementation is described. The validity of the proposed model is verified by various simulation results.**

Introduction

New advances in development of fast semiconductor switches and cost-effective DSP processors have revolutionized the adjustable speed motor drives. These new opportunities have contributed to the field of m otor drives by introducing novel configurations for electric machines in which the burden is shifted from complicated structures into software and control algorithms. This in turn has resulted in considerable improvement in cost while upgrading the performance of the overall drive system. Brushless DC (BLDC) is the most illustrating example for this trend [1]. Very compact geometry, an impressive efficiency along with a very simple control are among the main attractions for replacing many adjustable speed applications with this emerging technology.

Fundamentals of operation of BLDC motor drives are basically the same as seen in traditional permanent magnet brush dc motors in which field and armature switch places and an electronic commutator is employed to s witch the current from phase to phase. In order to achieve an optimal performance from the BLDC, the pulses of square- shaped armature current should be properly synchronized with the rotor position. This is referred to as field orientation in motor drive language. It is essential to note that, due to trapezoidal waveform of the induced motional Back-EMF in the armature circuit, a square- shape current waveform would result in a maximum torque density. Since the active contribution of magnetic structure in the process of torque development is relatively higher than other known motor drives, a more balanced and compact configuration is among advantages of BLDC as compared to other candidates. Moreover, the availability of high-energy permanent magnets like NdBrFe or SmCo has paved the way for development of highly efficient solutions for a variety of industrial and domestic applications such as aerospace, office products, automotive to name a few.

In order to cope with the increasing quest for BLDC drives, various design and control alternatives have been developed over the past two decades [2]- [3]. Although the design algorithms for BLDC drives are well established, developments of control and power electronic converters are far from exhausted. Problems such as high levels of torque pulsation, limited speed range, poor thermal performance and vulnerability to parameter variations in mass production are among the most challenging engineering issues that face this new technology. While some of these problems are inherent issues tied with the magnetic performance of the machine, reaching an overall optimality require a good understanding of the drive system performance. This is a common characteristic of new entities in motor drive market in which the integration o f various parts of the drive such as inverter, instrumentation, machine and control play a significant role. In fact an optimization in component level will not only result in suboptimal solutions but also can result in malfunction of the entire system. Th is has motivated many researchers to conduct researches on development of a tool for analysis of motor drive systems. Such a tool should offer a uniform analysis technique along with a modular structure in which various effects and sensitivity of different parts can be analyzed. Figure 1 shows such a configuration:

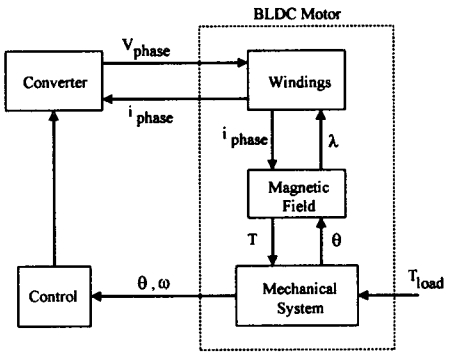

Fig. 1. Various components of the BLDC motor drive.

It is important to note that due to discontinuous nature of switching circuits along with nonlinear effects of magnetic circuit and mechanical system, development of a consistent model which can produce precise results in microscopic as well as in macroscopic scale in a timely fashion is not trivial. This is mainly due to the fact that circuit oriented programs are not suitable tools for simulation of differential equations governing the machine and its control. Lack of a user-friendly tool for modeling of switching circuits, on the other hand, has prohibited development of an overall model

of BLDC motor drive in system oriented programs. To overcome this obstacle, a new modeling tool for dynamic simulation of the switching networks seems to be a necessity. This will not only remove the limitation of having a generalized model of the drive system but also can be actively used for dimensioning and selection of power converter elements. Furthermore, considering the wide range of applications for BLDC motor drives, development of such an analytical tool in a user-friendly environment like Simulink/Matlab can be further sim plify the modeling of complex systems such as electric and hybrid electric vehicles where it can be used as a building block without considerable effort.

Therefore, in this paper, we propose a dynamic simulation model for an entire BLDC motor drive and its actual implementation. In this model, the trapezoidal back EMF waveforms are modeled as a function of rotor position, so that it can be actively calculated according to the operating speeds. Moreover, switching function concept is adopted to model the PWM inverter. This in turns results in obtaining the detailed voltage and current waveforms of the inverter and calculating the design parameters, such as average/rms ratings of components [4]. The developed model can produce precise prediction of drive performance during transient as well as steady state operation. Therefore, the mechanism of phase commutation and generation of torque ripple can be observed and analyzed in this model. Especially, the proposed model is made into several functional modular blocks, so that it can be easily extended to other ac motor applications with a little modification. Therefore, it is expected that the proposed model can be a robust solution for the development of BLDC motor drive. In the rest of this paper, the detailed explanation of the proposed model is presented and several informative simulation results are provided to verify the validity of the developed model.

Modeling and Implementation

In this section, the modeling approach is explained and the actual implementation using Matlab Simulink is described. Fig. 2 shows the overall block diagram of the developed model for BLDC motor drives. As shown in Fig. 2, the proposed model comprises of seven functional blocks namely, back EMF block, load current block, hysteresis current control block, PWM inverter block, diode rectifier block, pure switch and diode currents generating block, and speed/torque controller block.

Back EMF Block

The back EMF is a function of rotor position (θ_r) having the amplitude of $E = K_e \cdot \omega_r$ (K_e is back EMF constant). In this paper, the modeling of the back EMF is performed under the assumption, such that all three phases have identical back EMF waveforms. Based on the rotor position, the numerical expression of back EMF can be obtained and as an example, phase A back EMF can be expressed as eq. (1) and other phases can be obtained in the same manner. The actual implementation of the computed back EMF is shown in Fig. 3.

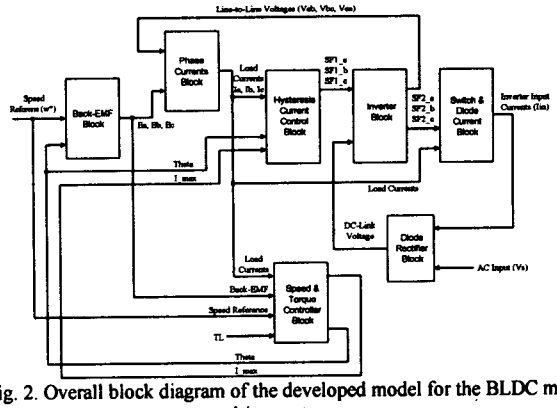

Fig. 2. Overall block diagram of the developed model for the BLDC motor drive systems.

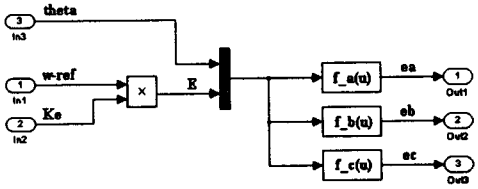

Fig. 3. Back EMF generating block from rotor positions.

$$e_a = \begin{cases} (6E/\pi)\theta_r & (0 < \theta_r < \pi/6) \\ E & (\pi/6 < \theta_r < 5\pi/6) \\ -(6E/\pi)\theta_r + 6E & (5\pi/6 < \theta_r < 7\pi/6) \\ -E & (7\pi/6 < \theta_r < 11\pi/6) \\ (6E/\pi)\theta_r - 12E & (11\pi/6 < \theta_r < 2\pi) \end{cases} \quad (1)$$

Therefore, with the speed command and rotor position, the symmetric three phases back EMF waveforms can be generated at every operating speed. In practical situation, due to manufacturing imperfection, deterioration of permanent magnets, or unbalanced stator windings, the back EMF waveforms become unbalanced. In this case, the real back EMF could be modeled using finite element analysis (FEA). Consequently, back EMF block can be modified by FEA program.

Speed and Torque Control Block

Speed and torque characteristics of the BLDC motor can be explained, neglecting the damping factor as

$$\omega_r = \frac{1}{J}\int (T_e - T_L)dt = \frac{1}{J}\int [(T_a + T_b + T_c) - T_L]dt \quad (2)$$

And, the relation between electrical power (P_e) and mechanical power (P_m) is

$$P_e = EI_{\max} = P_m = T_e\omega_r \quad (3)$$

Also, torque can be controlled very directly by varying the current amplitude as

$$T_e = \frac{E}{\omega_r} I_{\max} = K_t I_{\max}, \quad \left(K_t = \frac{E}{\omega_r} = \frac{K_e\omega_r}{\omega_r} \approx K_e\right) \quad (4)$$

where K_t is torque constant.

Therefore, using eqs. (2) to (4), the speed and torque control circuit can be implemented as shown in Fig. 4.

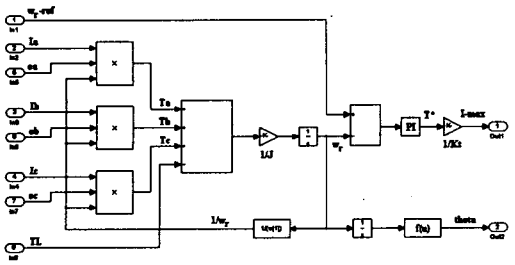

Fig. 4. Speed and torque control block.

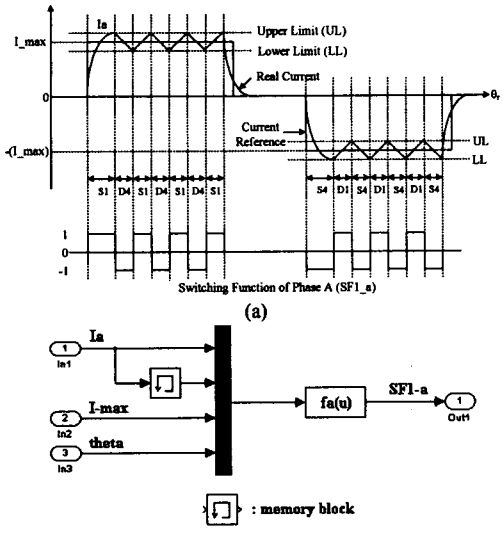

Fig. 5. (a) Detailed investigation of hysteresis current control for phase A, and (b) its implementation.

Hysteresis Current Control Block

In BLDC motor drive, duty-cycle controlled voltage PWM technique and hysteresis current control technique can be regarded as the main current control strategies. In this paper, bipolar hysteresis current control is used for obtaining the fast dynamic responses during transient states. This current control method is explained based for phase A. As shown in Fig. 5(a), current control for phase A can be divided into each four periods as followed by the polarity of the current. For example, in case of I_a>0

- Period 1: $I_a < Lower\ Limit(LL) \rightarrow$ Switch S_1 is turned on.
- Period 2: $I_a > Upper\ Limit(UL) \rightarrow$ Switch S_1 is turned off and D_4 is conducted.
- Period 3: $LL < Ia < UL$ *and* $dI_a / dt > 0 \rightarrow$ S_1 is turned on.
- Period 4: $LL < Ia < UL$ *and* $dI_a / dt < 0 \rightarrow$Switch S_1 is turned off and D_4 is conducted.

This hysteresis current control logic is realized in a function block $f_a(u)$ in cooperation with the measured phase A current I_a, current reference $I_{\_max}$, and rotor position θ_r as shown in Fig. 5(b).

From the hysteresis block, the switching function SF_{1_a}, SF_{1_b}, and SF_{1_c} are determined to model the operation of PWM inverter. The switching function concept is a powerful tool in understanding and optimizing the performance of the static power converters/inverters [4].

PWM Inverter, Load Current and Switch Current Blocks

In the BLDC, the only two phases are excited through the conduction operating modes. Therefore, the three phases currents are considered in terms of the line- to-line voltages. From Fig. 6, the following voltage and current equations can be obtained as

$$\begin{cases} v_{ab} = R_{LL} i_1 + (L-M)_{LL} \dfrac{di_1}{dt} + e_{ab} \\ v_{bc} = R_{LL} i_2 + (L-M)_{LL} \dfrac{di_2}{dt} + e_{bc} \\ v_{ca} = R_{LL} i_3 + (L-M)_{LL} \dfrac{di_3}{dt} + e_{ca} \end{cases} \quad (5)$$

where, LL designates line-to-line and $R_{LL} = 2R$ and $(L-M)_{LL} = 2(L-M)$.

And,

$$\begin{cases} i_a = i_1 - i_3 \\ i_b = i_2 - i_1 \\ i_c = i_3 - i_2 \end{cases} \quad (6)$$

Using switching function $SF_{1\_a,b,c}$, which is obtained from hysteresis block, the V_{ao}, V_{bo}, and V_{co} can be calculated as

$$\begin{cases} v_{ao} = \dfrac{V_d}{2} SF_{1\_a} = \dfrac{V_d}{2} \sum_0^\infty A_n \sin(n\omega t) \\ v_{bo} = \dfrac{V_d}{2} SF_{1\_b} = \dfrac{V_d}{2} \sum_0^\infty A_n \sin n(\omega t - 120^\circ) \\ v_{co} = \dfrac{V_d}{2} SF_{1\_c} = \dfrac{V_d}{2} \sum_0^\infty A_n \sin n(\omega t - 240^\circ) \end{cases} \quad (7)$$

Then, the inverter line-to-line voltages can be derived as

$$\begin{cases} v_{ab} = v_{ao} - v_{bo} = \dfrac{V_d}{2}(SF_{1\_a} - SF_{1\_b}) \\ v_{bc} = v_{bo} - v_{co} = \dfrac{V_d}{2}(SF_{1\_b} - SF_{1\_c}) \\ v_{ca} = v_{co} - v_{ao} = \dfrac{V_d}{2}(SF_{1\_c} - SF_{1\_a}) \end{cases} \quad (8)$$

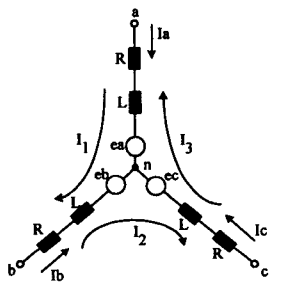

Fig. 6. Voltage and current parameters in a three-phase BLDC motor.

From the calculated phase currents, the detailed pure switch and diode currents are derived using switching function SF_2. Each phase has two switching functions of

SF_2, such as SF_{2_S1} and SF_{2_S4} for switches S_1 and S_4, respectively with the following definition as

$$\begin{cases} SF_{2\_S1} = SF_{1\_a} > 0 \\ SF_{2\_S4} = SF_{1\_a} < 0 \end{cases} \quad (9)$$

Based on the eq. (9) and Fig. 5(a), the switch and diode currents for phase A are calculated as

$$\begin{cases} I_{S1\_S} = (I_a > 0) \cdot SF_{2\_S1} \\ I_{S1\_D} = (I_a < 0) \cdot SF_{2\_S1} \\ I_{S4\_S} = (I_a < 0) \cdot SF_{2\_S4} \\ I_{S1\_D} = (I_a > 0) \cdot SF_{2\_S4} \end{cases} \quad (10)$$

where, I_{S1_S} and I_{S1_D} are pure switch and diode currents of switch S_1 as $I_{S1} = I_{S1\_S} - I_{S1\_D}$.

Also, the inverter input current (I_{in}) can be obtained by

$$I_{in} = I_{S1} + I_{S3} + I_{S5} \quad (11)$$

The implementations of the above-explained numerical PWM inverter voltage and current equations are shown in Figs. 7, 8, and 9. Consequently, from the inverter, load current, and switch/diode blocks, all voltage and current variables of the PWM inverter can be obtained.

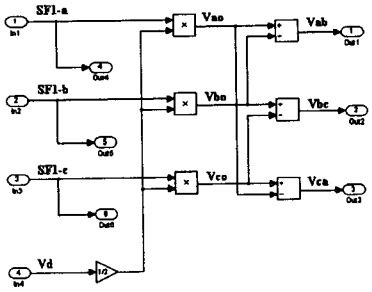

Fig. 7. Inverter line-to-line voltage generating block using switching functions.

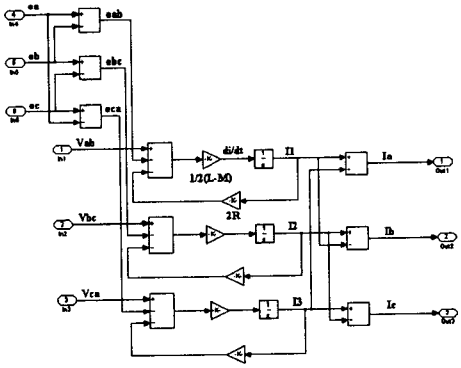

Fig. 8. Implementation of three-phase currents block.

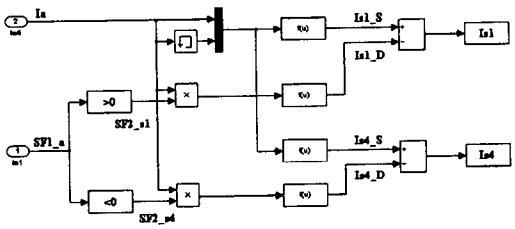

Fig. 9. Pure switch and diode currents generating block for phase A.

Simulation Results

Table I shows the specifications of the experimental BLDC motor drive used in this study. Fig. 10 shows the generated back EMF from the rotor position and the phase currents waveforms at 2500[rpm]. Also, the actual phase currents are successfully obtained by the hysteresis control algorithm and they are well synchronized with their counterpart back EMF waveforms. Fig. 11 shows the dynamic responses of the speed and torque controller, which is designed as shown in Fig. 4.

Table I Motor Specification (LL: line-to-line)

K_t	0.21476[Nm]	R_{LL}	1.5[Ω]
$K_{e\ LL}$	0.21486 [V/(rad/sec)]	$(L\text{-}M)_{LL}$	6.1[mH]
J	8.2614e-5[kgm^2]	Power	1[HP]
T_L	0.662[Nm]	Rated Speed	3500[rpm]

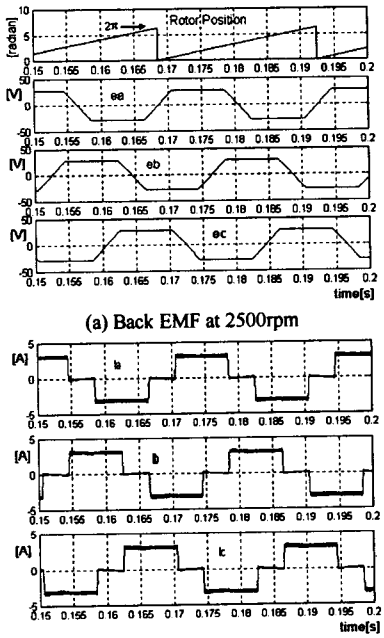

(a) Back EMF at 2500rpm

(b) Phase currents at 2500rpm

Fig. 10. Computation of back EMF and current profiles based on the rotor positions.

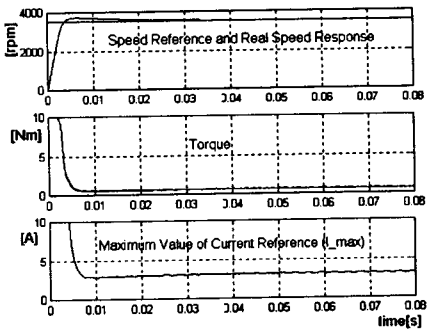

Fig. 11. Dynamic responses of speed and torque controllers.

Detailed operational characteristics of the PWM inverter are examined in Figs. 12 and 13. As explained earlier, the

PWM inverter modeling is based on switching function concept. Figs. 12(a) shows the switching function SF_1. From the figures, it is noted that the switching function signals are only generated during the 120° conduction periods in order to force the currents to be switched between the hysteresis upper and lower bands. The positive (negative) value 1 (-1) expresses the upper (lower) switch or diode is under the conducting state. Therefore, from the switching function SF_1, the line-to-line voltage waveforms can be obtained as shown in Fig. 12(b). In case of Fig. 12(b), phase A current is positive and phase B current is negative. Therefore, during positive slope of phase A ($d_{ia}/dt>0$) and negative slope of phase B ($d_{ib}/dt<0$), switches S_1 and S_6 are conducted, so that V_{ab} has positive value of V_d (160V).

In order to obtain the optimal design parameters of the PWM inverter, the pure switch and diode current waveforms are necessary for calculating the average and rms values. They also can be obtained from the combination of the phase currents and switching function SF_2. Fig. 13 explains the detailed process of calculating the pure switch and diode currents.

Conclusions

In this paper, a dynamic simulation model of the BLDC motor drives has been proposed and its actual implementation is presented by using Matlab Simulink. The advantages of this model comparing with the conventional simulation models have been recognized. Therefore, it is expected that the proposed model can be a robust design tool and be effectively utilized to develop the power conversion circuits and control strategies for the BLDC motor drives.

References

[1]. J. R. Hendershot and T. J. E. Miller, *Design of brushless permanent-magnet motor*, Oxford, 1994.

[2]. P. Pillay and R. Krishnan, "Modeling, simulation, and analysis of permanent-magnet motor drives, Part II: the brushless dc motor drive," *IEEE Trans. Ind. Applicat.*, vol. 25, no. 2, pp. 274-279, March/April 1989.

[3]. P. D. Evans and D. Brown, "Simulation of brushless dc drives," in *IEE Proc.*, vol. 137, no. 5, pp. 299-308, September 1990.

[4]. B. K. Lee and M. Ehsani, "A simplified functional model for 3-phase voltage-source inverter using switching function concept," *IEEE Trans. Ind. Electron*, vol. 48, no. 2, pp. 309-321, April 2001.

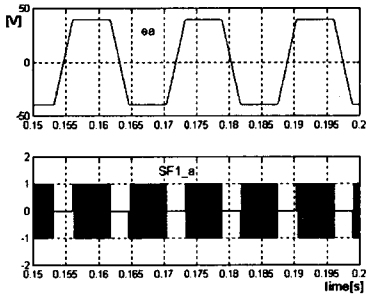

(a) Back EMF and switching function for phase A.

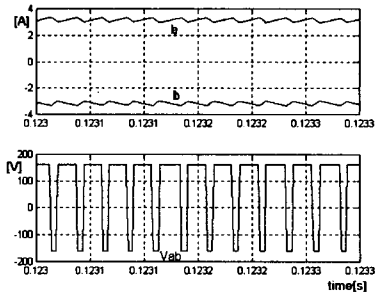

(b) Line-to-line voltage V_{ab} ($I_a>0$, $I_b<0$)

Fig. 12. Switching function $SF_{1\_a,b,c}$ and line-to-line voltage (V_{ab}) waveforms according to the conducting modes.

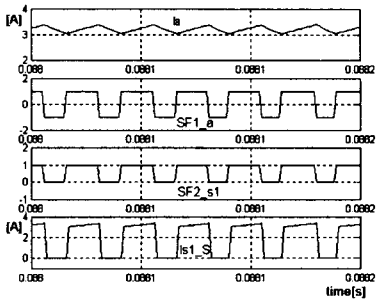

(a) Pure switch current I_{s1_S} ($I_a>0$)

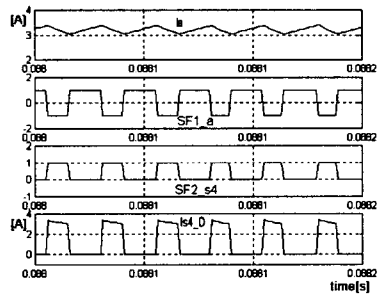

(b) Pure diode currents I_{s4_D} ($I_a>0$)

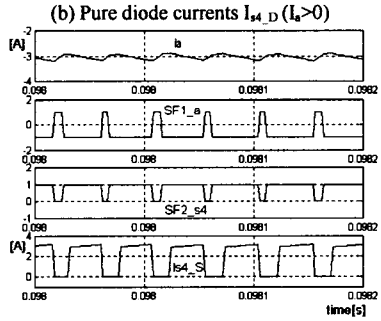

(c) Pure switch current I_{s4_S} ($I_a<0$)

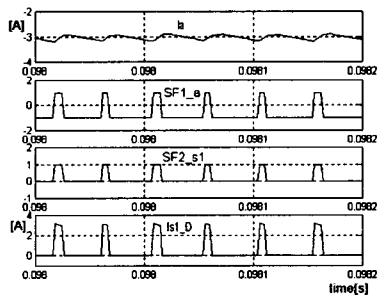

(d) Pure diode currents I_{s1_D} ($I_a<0$)

Fig. 13. Pure switch and diode current waveforms of switch S_1 and S_4.